

Exploring the origins of crystallisation kinetics in hierarchical materials using *in situ* X-ray diffraction and Pair distribution function

Matthew E. Potter,^a Mark E. Light,^{*a} Daniel J. M. Irving,^a Alice E. Oakley,^a Stephanie Chapman,^a Philip Chater,^b Geoff Cutts,^b Andrew Watts,^b Michael Wharmby,^b Bart D. Vandegehuchte,^c Moritz Schreiber^c and Robert Raja^a

^a University of Southampton, Chemistry Department, Southampton, Hants, SO17 1BJ, UK. E-mail: light@soton.ac.uk

^b Diamond Light Source, Harwell Science and Innovation Campus, Didcot, Oxon, OX11 0DE, UK

^c Total Research & Technology Feluy, Zone Industrielle Feluy C, B-7181 Seneffe, Belgium

Experimental

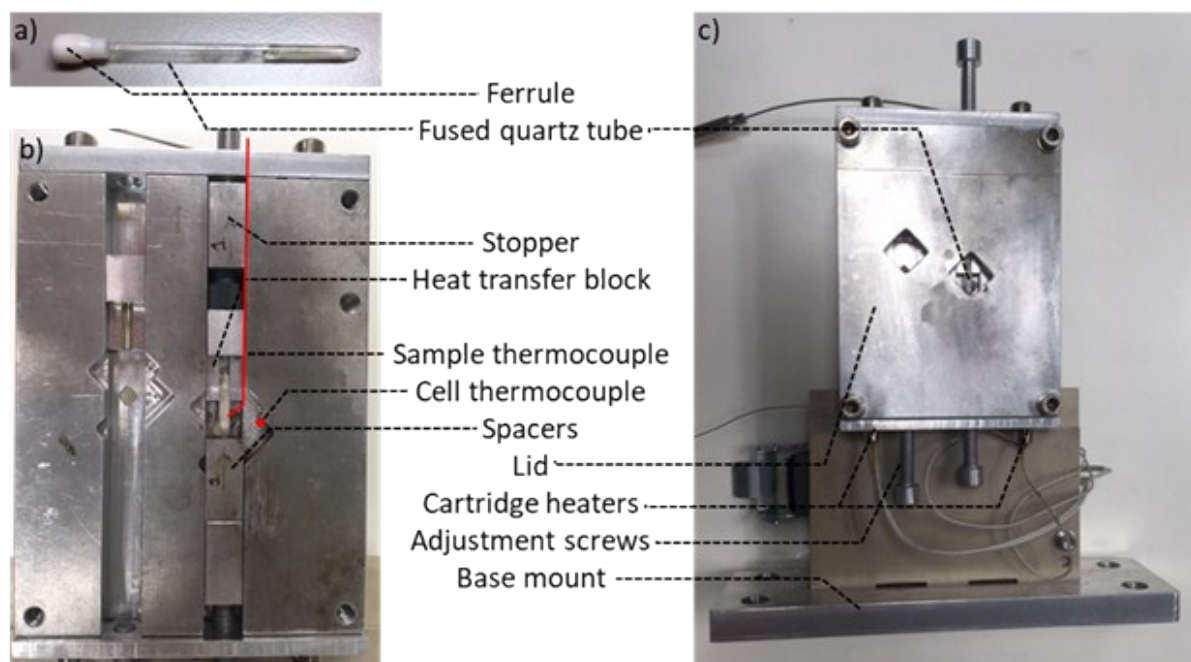


Figure S1: Details of the I15-1 hydrothermal cell. a) Fused quartz tube with Teflon ferrule attached and sample sealed inside. b) Inside the hydrothermal cell, showing two vertical channels where samples can be loaded. One channel is loaded with a sample, heat transfer block and aluminium spaces to align the sample to the upstream window (behind the tube). The sample thermocouple (indicated as a red line) runs underneath the heat transfer blocks until close to the beam position, where it is bent so that the tip of the thermocouple is pressed against the sample tube. The cell thermocouple (position indicated as a red dot) is secured into the back of the cell so that it can not become disconnected during operation. c) Fully assembled hydrothermal cell with the lid attached. The diamond-shaped downstream windows allow the scattered X-rays to leave the cell unimpeded.

Powdered HP and MP AlPO-5 *ex situ* synthesis

6.84 mL of H₃PO₄ (85 wt. % in water) was diluted in 30 mL of deionised water and stirred in a Teflon beaker. 20.43 g of group aluminium hydroxide was gradually added to the diluted acid and left to stir for 1.5 hours. 8.07 mL of dimethyloctadecyl[3-(trimethylsilyl)propyl] ammonium chloride (DMOD) (42 wt.% in water, this was emitted for the MP AlPO-5 system) was added dropwise to the reaction

mixture, followed by 11.16 mL of triethylamine, followed by a further 15 mL of deionised water. The gel mixture stirred for a further 1.5 hours before being distributed between twelve Teflon lined 30 mL stainless steel autoclaves with a small proportion of the gel being retained and labelled t=0.

The autoclaves were sealed and transferred to a preheated fan-assisted oven at 200 °C. After 2 hours of heating one autoclave was removed from the oven and immediately quenched in ice and labelled t=2 hours. This was repeated after 24 hours of heating to produced sample t=24 hours. The products from each autoclave were isolated *via* vacuum filtration, washed with 500 mL of deionised water and allowed to dry overnight at 70 °C under air. Calcination of the samples was achieved in a tube furnace under a flow of air for 16 hours at 600 °C with a heating ramp rate of 5 °C min⁻¹. Total scattering measurements were carried out on the t=0 gel, as well as the powdered HP AlPO-5 samples at t=2 hours and t=24 hours both before and after calcination.

***Ex situ* PDF experiments carried out at University of Southampton**

In-house total scattering data were collected on a *Rigaku R-Axis 3-circle Spider* goniometer equipped with a curved Fujifilm image plate mounted at the window of a graphite monochromated sealed silver tube (Ag K α 1/K α 2 = 0.560886 Å) operating at 2.0 kW (40kV, 30mA). The sample was mounted in a 2 mm OD borosilicate capillary and placed at a fixed distance of 127.4mm from the detector (achievable Q_{max} for this geometry is 22 Å⁻¹). Exposures for the empty diffractometer (background), the empty capillary (container) and the full capillary (sample) were made with matched times of either 60 minutes for crystalline material or 180 minutes for liquids; the samples were oscillated through a ϕ angle of 160 ° during the measurements.

Image plate data were converted to 1D profiles using 2DP^[S1] and converted to PDFs using GudrunX.^[S2]

***Ex situ* powder X-ray diffraction carried out at University of Southampton**

Phase purity and crystallinity of materials was confirmed by powder X-ray diffraction. Powder X-ray diffraction (PXD) was performed on a Bruker D2 Phaser diffractometer with Cu K α 1 radiation. Patterns were run over a 2 θ range of 5–60 ° with a scan speed of 3 °/min and an increment of 0.01 °.

N₂ physisorption measurements

BET surface area measurements were performed at 77 K, on a sample dried under 20 mTorr of vacuum at 120 °C overnight. Analysis was performed on a Micromeritics Gemini 2375 surface area analyzer. Surface area was calculated using the BET model.

Physicochemical characterisation of *ex situ* samples

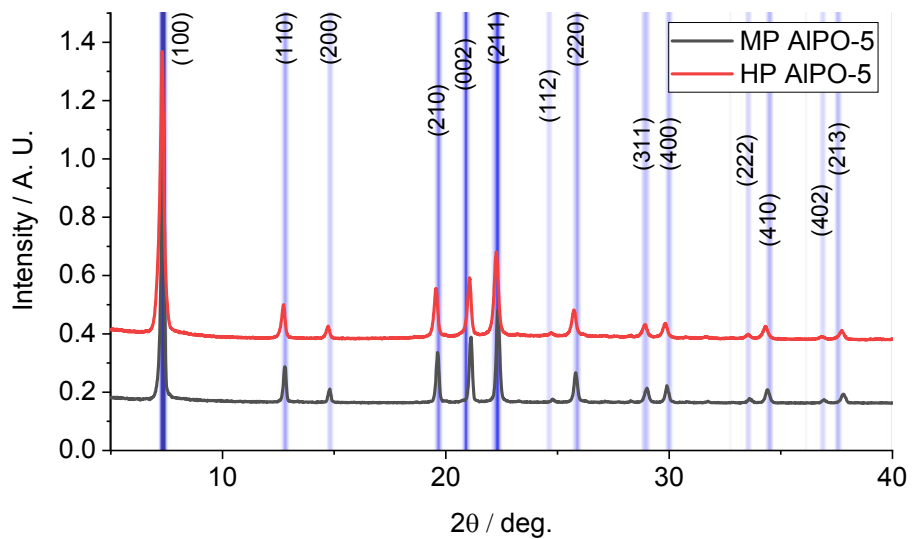


Figure S2: *Ex situ* powder X-ray diffraction data of calcined HP and MP AIPO-5 with Cu K α radiation ($\lambda = 1.5406 \text{ \AA}$), confirming the phase purity of the system and validating our synthesis protocol. Calculated pattern with main lines indexed is shown as a pseudo-film pattern in the background.

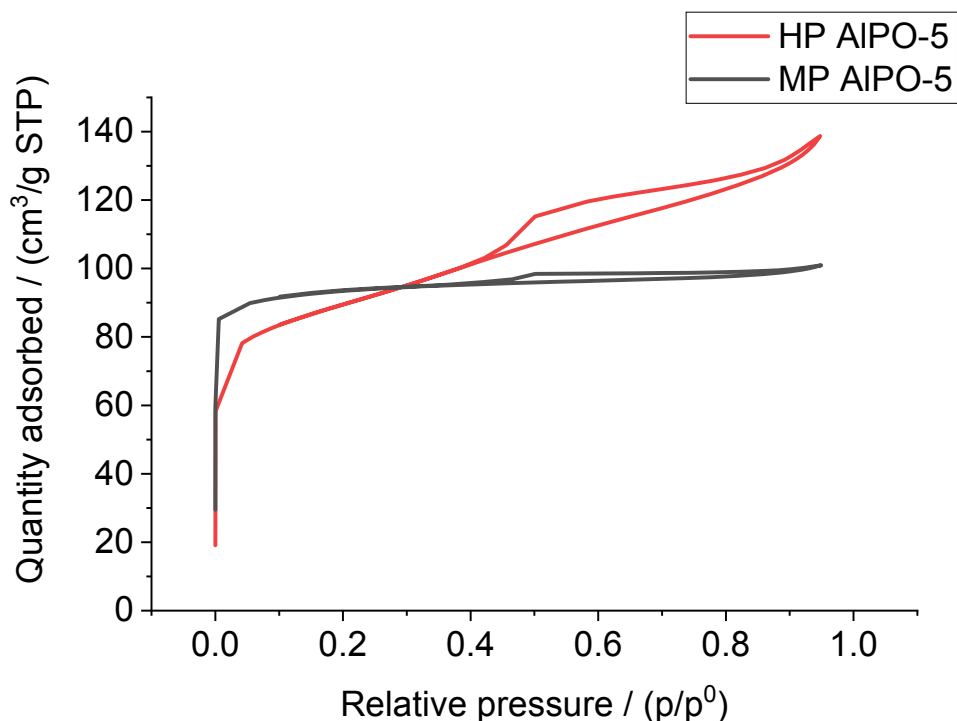


Figure S3: N₂ physisorption isotherms at 77 K, showing a typical microporous isotherm (MP AIPO-5), and a type IV hysteresis signifying the hierarchical nature of HP AIPO-5.

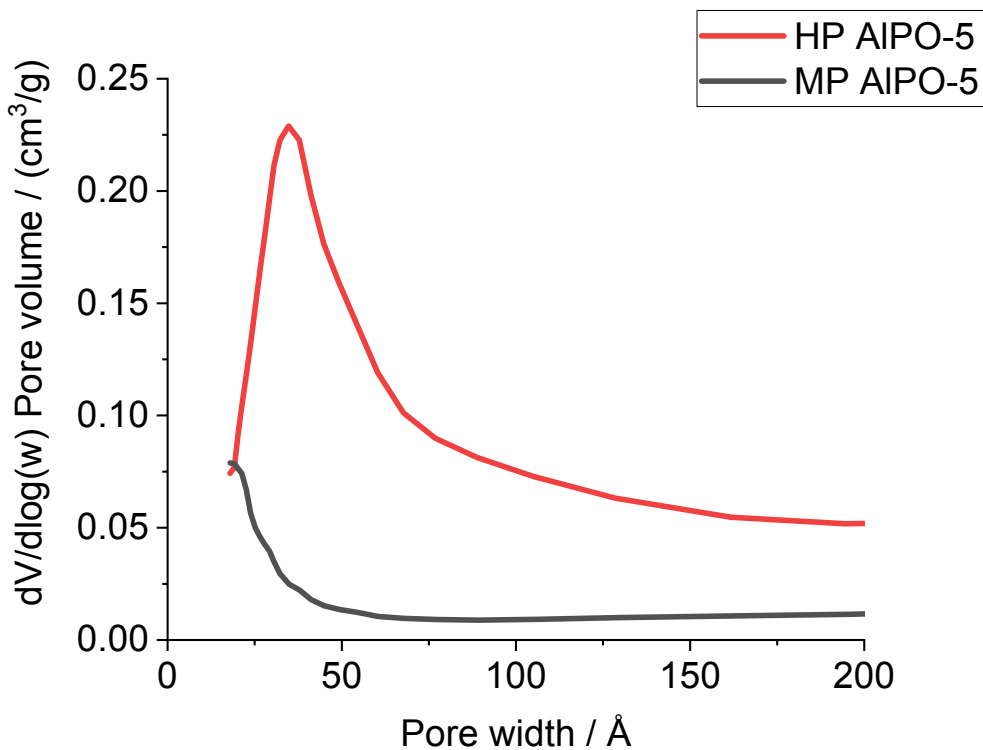
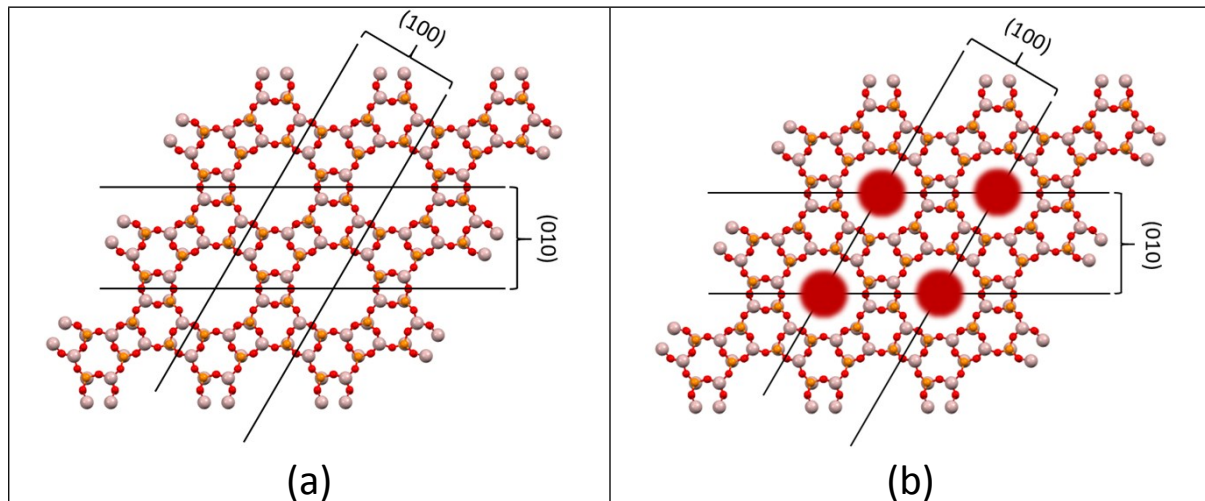


Figure S4: BJH pore-distribution plots showing the presence of mesopores in HP AIPO-5, and the absence of them in the microporous MP AIPO-5 species.

Simulated channel filling of AIPO-5 XRD data

Both models, AIPO-5 (a) and AIPO-5 + channel structure directing agent (SDA) (b), were based on the atomic coordinates from Qiu^[S3] *et al.* and the diffraction patterns generated using CrystalDiffract versions 6.8.2^[S4]. For AIPO-5 + channel SDA - carbon atoms were included at various coordinates within the channels to crudely simulate electron density from residual structure directing agent and the diffraction pattern recalculated.



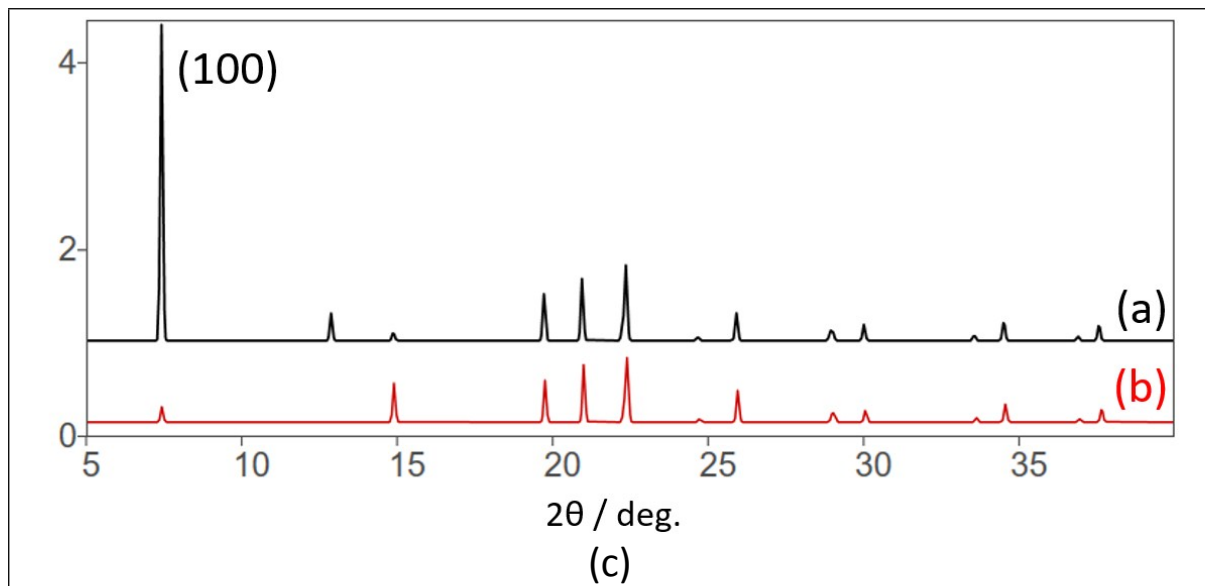


Figure S5: Simulated XRD patterns with Cu K α radiation ($\lambda = 1.5406 \text{ \AA}$), of AlPO-5 with empty channels (a) and filled channels (b) highlighting the influence on the scattering intensity as seen in the first Bragg peak (100), due to reduced electron density contrast.

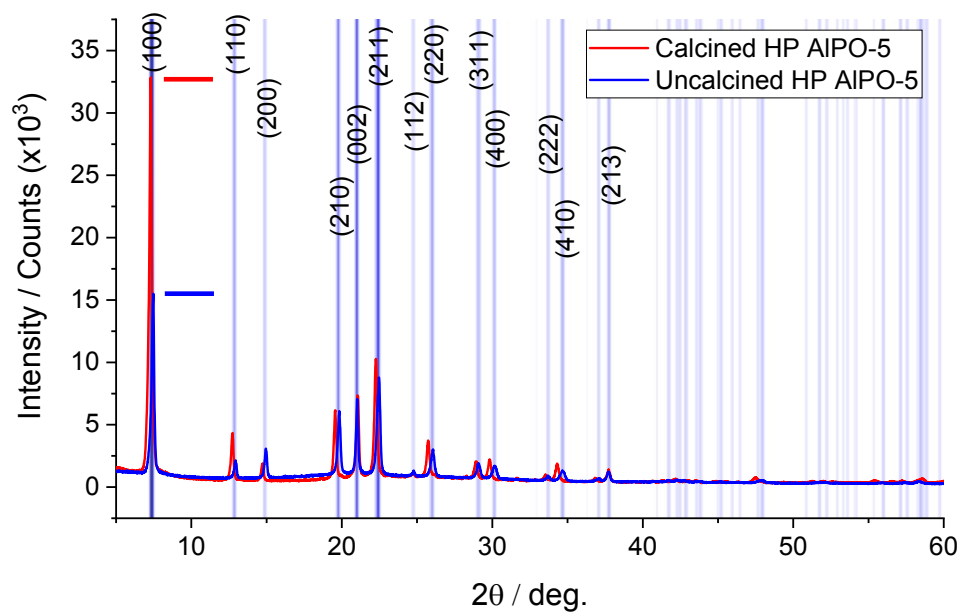


Figure S6: Comparing the intensity of the (100) peak in calcined and uncalcined HP AlPO-5, with powder XRD, using Cu K α radiation ($\lambda = 1.5406 \text{ \AA}$), showing the (100) peak intensity is heavily influenced by the presence of the template. However other peaks, particularly the triplet (19 – 23 °) is barely influenced. Calculated pattern with main lines indexed is shown as a pseudo-film pattern in the background.

Total scattering data

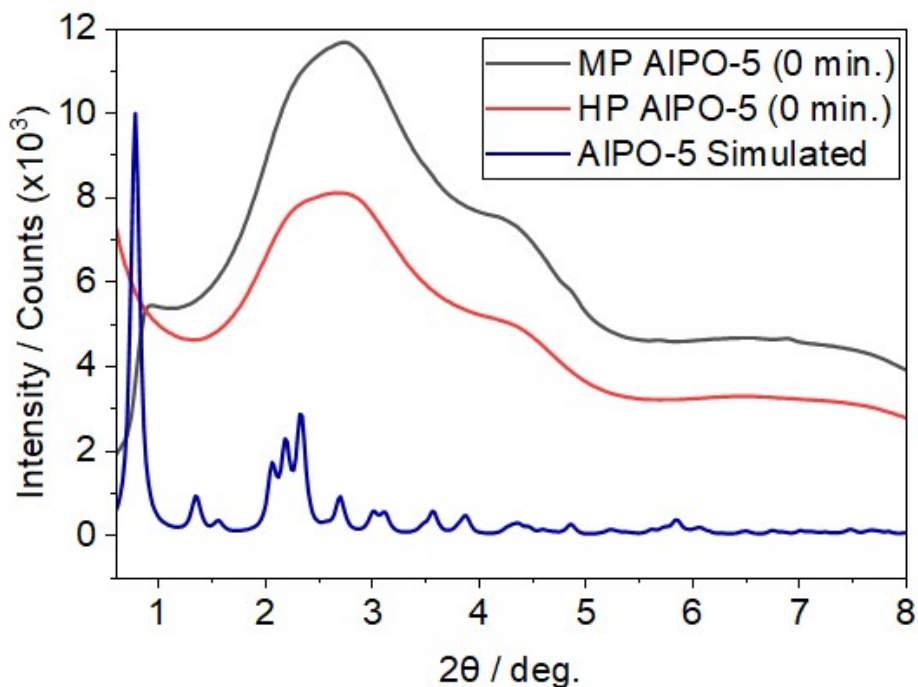


Figure S7: Comparing *in situ* total scattering data of MP (black) and HP (red) AIPO-5 synthesis gels at room temperature (0 minutes), prior to heating, showing differences in scattering intensity for the two systems. Recorded at

Pair distribution function data

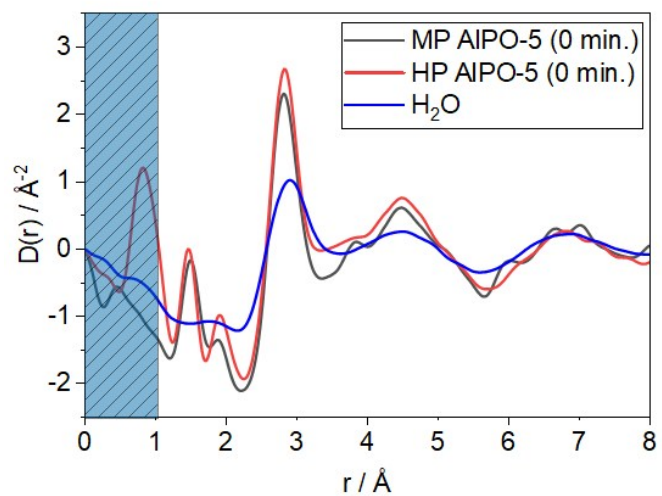


Figure S8: Comparing the *in situ* PDF data of MP (black) and HP AIPO-5 (red) synthesis gels at room temperature, contrasting with *ex situ* H₂O data (blue) collected at Southampton. Again, MP and HP AIPO-5 show excellent agreement, with the exception of $r < 1 \text{ \AA}$, which are likely artefacts of the PDF analysis.

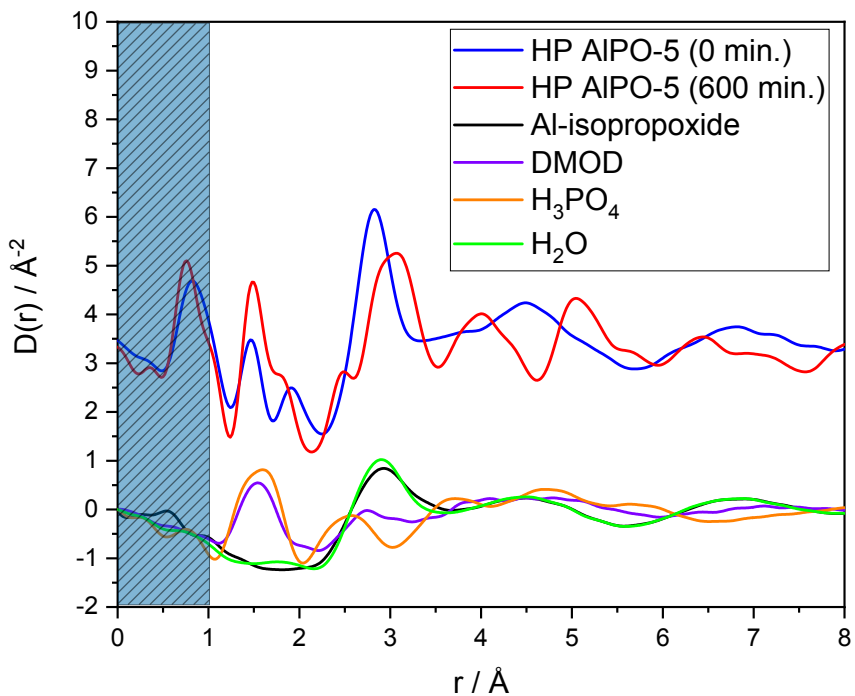


Figure S9: Comparing the *in situ* PDF data of HP AlPO-5 prior and post crystallisation (0 and 600 min respectively), with PDF data of isolated synthesis precursors measured *ex situ* at Southampton. This shows the strong contribution of water to the *in situ* HP AlPO-5 data.

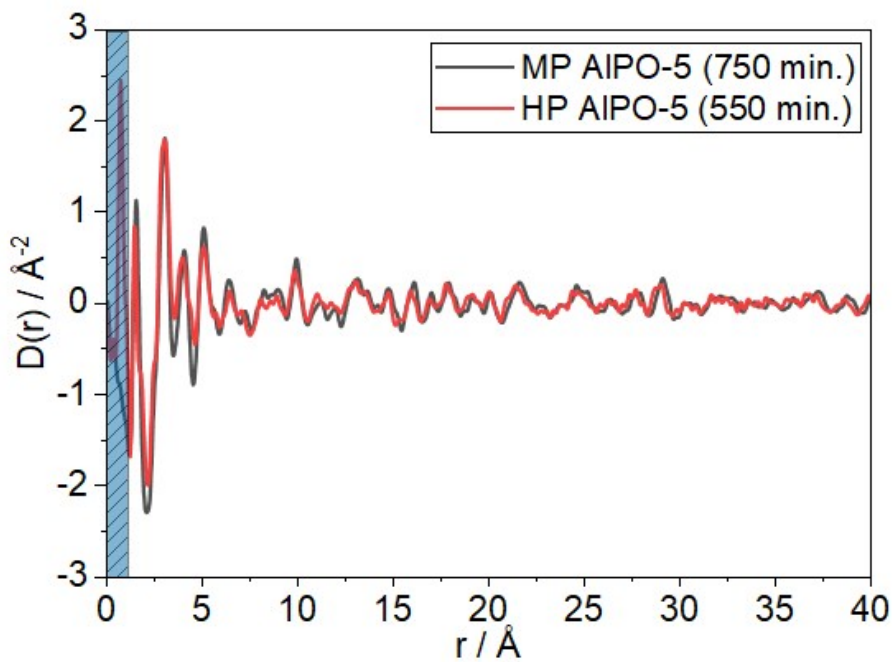


Figure S10: Comparison of *in situ* PDF data for MP (black) and HP AlPO-5 (red) after crystallisation completion showing similarity, along range order to high r .

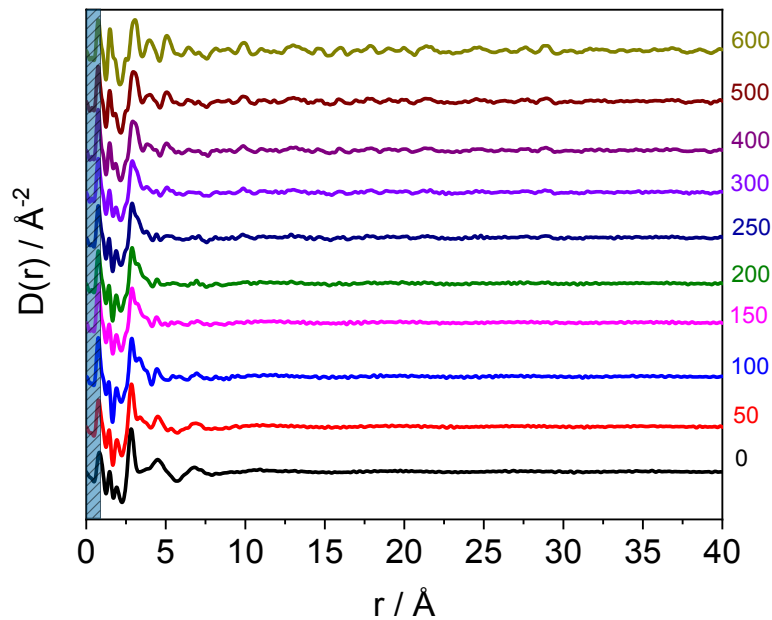


Figure S11: Stacked *in situ* PDF data for HP AlPO-5 during crystallisation, showing the evolution of long-range order after 200 minutes (100 minutes at 200 °C).

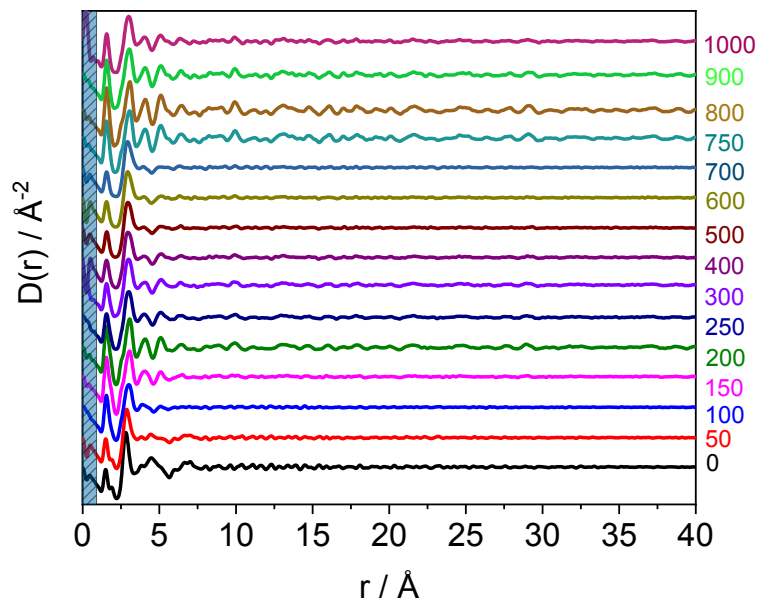


Figure S12: Stacked *in situ* PDF data for MP AlPO-5 during crystallisation, showing the evolution of long-range order after 200 minutes (100 minutes at 200 °C).

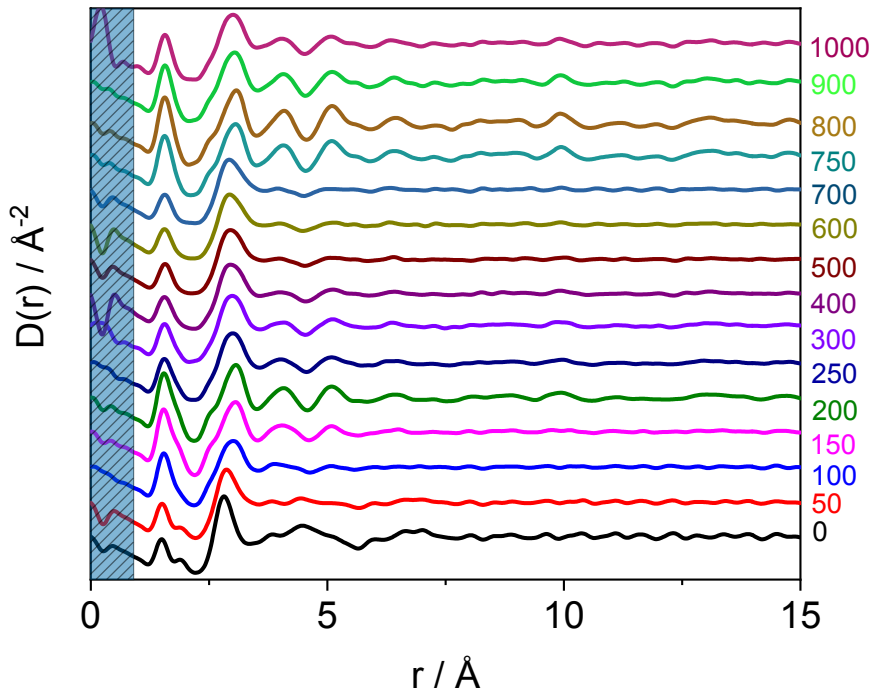


Figure S13: Stacked *in situ* PDF data (zoomed) for MP AlPO-5 during crystallisation, showing the evolution of long-range order after 200 minutes (100 minutes at 200 °C).

PDF Data Reduction ^[S5,S6]

PDF data; $D(r)$, can be obtained from raw high-powered X-ray or neutron data, $I(Q)$, where Q is the scattering vector, defined by:

$$Q = \frac{4\pi \sin \theta}{\lambda}$$

Processing measured total scattering data intensities, $I_m(Q)$, to the final PDF involves well-documented processing, normalization and correction of data in order to obtain a true and representative PDF of the material.

$$I_m(Q) = a(Q)I_c(Q) + b(Q)$$

Where $I_c(Q)$ is the coherent and corrected intensity, and $a(Q)$ and $b(Q)$ represent the multiplicative and addition corrections respectively. These corrections must be carefully applied to allow for the final data to be truly representative of the material being analysed. It is important to note that these corrections do not remove data essential to the structure, but rather those corrections to fundamental physical and instrumental factors. Examples of multiplicative corrections; $a(Q)$, include beam polarization, which varies with the source and instrument set-up, other factors also include the self-absorption within the sample. Additive corrections; $b(Q)$ include removal of unrelated scattering such as that from the background and container, as well as removal of dead pixels from the detector. Other factors also include that of physical effects such as Compton and fluorescence events. With careful removal of these factors, the coherent and corrected intensity, $I_c(Q)$ can be used to transform the data into a normalized total-scattering structure function, $S(Q)$. This is as follows:

$$S(Q) = \frac{I_c(Q) - \langle f(Q)^2 \rangle + \langle f(Q) \rangle^2}{\langle f(Q) \rangle^2}$$

Where $f(Q)$ is the atomic scattering factor with the pointed brackets being used to show the average of said atomic scattering factors over all atoms present in the samples. This total-scattering structure function can then be reduced to the reduced total-scattering structure function, $F(Q)$.³²

$$F(Q) = Q[S(Q) - 1]$$

From this, the data undergoes a Fourier transformation to obtain the final PDF, $D(r)$:

$$D(r) = 4\pi r(\rho(r) - \rho_0) = \frac{2}{\pi} \int_{Q_{min}}^{Q_{max}} Q[S(Q) - 1] \sin(Qr) dQ$$

The PDF, $D(r)$, can then be compared with simulated patterns of both full structures or fragments, calculated from periodic or molecular coordinates respectively by:

$$D(r) = \frac{1}{r} \sum_{ij} \frac{b_i b_j}{\langle b \rangle^2} \delta(r - r_{ij}) - 4\pi\rho_0$$

where the sum of all atoms within the material, r_{ij} is the distance between atoms i and j respectively. b_i is the scattering length of the atom I, and $\langle b \rangle$ is the average scattering length of the sample.

References

- S1) 2DP Version 2.0.1.1, Rigaku Corporation (2007-2013)
- S2) A. K. Soper and E. R. Barney, *J. Appl. Cryst.*, 2011, **4**, 714-726.
- S3) S. Qiu, W. Pang, H. Kessler and J. L. Guth, *Zeolites*, 1989, **9**, 440–444.
- S4) D.C. Palmer, CrystalMaker. CrystalMaker Software Ltd, Begbroke, Oxfordshire, England, 2019.
- S5) T. Egami and S. Billinge, *Underneath the Bragg Peaks*, Elsevier, Amsterdam, 2nd Edition, 2012.
- S6) P. Juhás, T. Davis, C. L. Farrow and S. J. L. Billinge, *J. Appl. Crystallogr.*, 2013, **46**, 560–566.